

# Electron-magnon diffusion and magnetization reversal detection in FePt thin films

A. P. Mihai, J. P. Attané,\* A. Marty, P. Warin, and Y. Samson  
 DRFMC/CEA Grenoble, 17 avenue des Martyrs, 38054 Grenoble Cedex 9, France  
 (Received 17 December 2007; published 7 February 2008)

We measured the dependence of the electrical resistivity on perpendicular magnetic field in FePt(10–32 nm)/MgO layers from 3 to 300 K. We show that the magnetoresistance is proportional to both the perpendicular magnetization of the FePt layer and the perpendicular applied field. Building on previous models, we show that this magnetoresistance can be ascribed to electron-magnon interactions, giving a linear dependence of resistivity upon magnetization in the limit of a low field to magnetocrystalline anisotropy ratio. This magnetoresistance effect can be used to follow magnetization reversal in certain conditions, with perspectives that we discuss with respect to other magnetoresistive effects.

DOI: [10.1103/PhysRevB.77.060401](https://doi.org/10.1103/PhysRevB.77.060401)

PACS number(s): 75.30.Ds, 72.10.Di, 72.25.Ba, 85.75.-d

The development of spintronics is based upon a few electronic spin-dependent transport properties, mainly anisotropy magnetoresistance (AMR),<sup>1</sup> giant magnetoresistance (GMR),<sup>2</sup> and tunneling magnetoresistance (TMR),<sup>3</sup> and at a lower level the anomalous Hall effect (AHE) and intrinsic domain wall resistivity<sup>4</sup> (DWR) (see Refs. 5–7 for review articles). These magnetoresistive effects paved the way for high-impact technological devices such as the hard-disk recording head or the emerging magnetic random access memories. In addition, the basic understanding of magnetization reversal phenomena in nanometer-scale elements hugely benefited from such versatile electrical effects, providing sensitive and ultrafast tools for magnetization detection.

Here, we measure the electrical resistivity of FePt thin films with perpendicular magnetization, resulting from the huge perpendicular magnetocrystalline anisotropy induced by uniaxial chemical ordering in the *L10* phase. Such thin films exhibit full magnetic remanence, implying that the magnetization state is unchanged from high fields collinear to the magnetization down to the value of the negative field corresponding to magnetization reversal. We then observed that the contribution of magnon scattering to the electrical resistivity provides a linear dependence of the resistance on the applied field, but also gives rise to a clear magnetoresistance effect, in which the recorded resistivity is proportional to the perpendicular magnetization of the thin magnetic layer. This effect—which could be named magnon magnetoresistance (MMR)—is thus an additional tool to detect and follow magnetization reversal. In 2002, Raquet *et al.*<sup>12</sup> showed that the magnon-electron interactions are the source of a linear dependence of the resistivity on a high applied field. This was observed in the high-field region (well above magnetization saturation) for 3*d*-metal thin films, and the theoretical analysis of the authors provided the basis from which we extended our analysis. In order to avoid the mixing of AMR and DWR contributions in the low-field regime, we used high-anisotropy FePt layers having full magnetic remanence.

Epitaxial FePt/MgO(001) films, chemically ordered in the *L10* structure, were grown by molecular-beam epitaxy as described previously.<sup>8</sup> Due to the very high magnetocrystalline anisotropy of the FePt alloy ( $K_u = 5 \times 10^6$  J/m<sup>3</sup>), these

thin films exhibit desirable magnetic properties: thin (4 nm) Bloch domain walls (DWs), magnetization reversal occurring through DW propagation.<sup>9–11</sup> In 10-nm-thick samples, the hysteresis loop [see Fig. 1(a)] shows a sharp magnetization reversal and the coercive field ranges between 0.3 and 0.5 T.

Room temperature anomalous Hall effect and resistivity measurements were performed on a very sensitive electrical transport setup using lock-in techniques, with an external magnetic field applied perpendicularly to the layer, and ranging from –1.2 to 1.2 T. Both the AHE and the corresponding resistivity measurements are presented in Fig. 1. A sharp decrease in resistivity, of about 0.17%, is noticed at the coercive field, in both positive and negative half loops, this decrease being clearly related to the magnetization reversal. Also, when the sample is magnetically saturated, one can see a linear variation of the resistivity with the applied field.

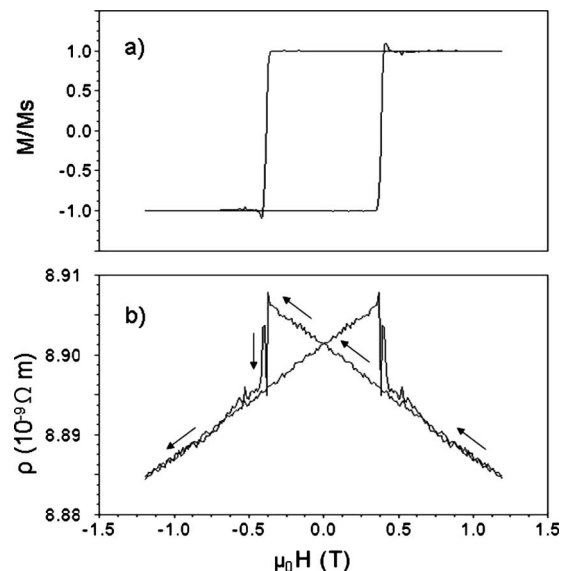


FIG. 1. (a) Hysteresis loop measured in perpendicular field by anomalous Hall effect and (b) corresponding resistivity measurement, performed on an FePt(10 nm)/MgO(001) sample. The measurement has been done using the six-probe technique. The data have been symmetrized and antisymmetrized, respectively, to separate properly the MR and AHE contributions.

This linear, nonsaturating negative magnetoresistance at high fields, corresponding to the magnetically saturated state, has already been reported for high in-plane applied fields in 3d ferromagnetic layers.<sup>12</sup> This resistivity decrease was assigned to spin-wave damping in high fields, which corresponds to a decrease of the intrinsic spin disorder. The field increase thus leads to a diminishing of the electron-magnon scattering.

In our measurements we observe a similar linear dependence of the MR on the applied magnetic field for low positive fields, and even for negative applied fields (see Fig. 1), i.e., in the state where magnetization and applied field are antiparallel. To understand this unexpected behavior, one has to take into account the specific magnetic properties of our FePt thin film. Qualitatively, when the applied field and magnetization directions are antiparallel, the high-anisotropy field tends to maintain the magnetization direction, while the applied field tends to destabilize it, thus increasing the magnon population. As a result, when the magnetization and applied field are antiparallel, a linear increase of the resistance with the field absolute value can be observed.

When the coercive field is attained, the magnetization switches from a saturated state to the opposite one, and the relative orientation of the applied field and the magnetization switches from antiparallel to parallel. This leads to a sudden decrease of the magnon population and thus to the observed fall of resistivity.

To support this qualitative explanation, we derived, from the work of Raquet *et al.*,<sup>12</sup> an electron-magnon scattering model for low applied fields, which takes into account the large anisotropy field encountered in our samples.

The resistivity of a ferromagnetic material is basically the sum of two terms, a magnetic term and a nonmagnetic term. The nonmagnetic term (phonons, impurities, and so on) is supposed to be weakly dependent on the applied field in the saturated state. On the other hand, the magnetic term is highly dependent on the applied magnetic field and contains three main contributions to the resistivity: the intrinsic DWR, the AMR (including that arising from the DWs), and the magnon magnetoresistance. Due to the fact that, in the saturated state, there are no DWs, and that during our measurement the magnetization  $M$  and the current are in perpendicular directions, the first two magnetic contributions to the resistivity are negligible: In the sample of Fig. 1, the observed resistivity variations correspond simply to the MMR contribution.

The model developed by Raquet *et al.*<sup>12</sup> on the ground of Goodings' work<sup>13</sup> is based on the assumption that the magnetic field mainly affects spin-flip electronic processes. Two spherical energy  $s$  and  $d$  bands are assumed, for which  $s$ - $d$  transitions require spin waves whose wave vectors  $q$  exceed the radial distance between the two Fermi spheres of radius  $K_{Fs}$  and  $K_{Fd}$ . The probability of spin-flip transition between the two bands is closely related to the energy spectrum of the magnons involved in such a transition. In the approximation of long-wavelength magnons, the dispersion relation of magnons has a quadratic form,<sup>14</sup>

$$E(q) = Dq^2 + g\mu_B B_t, \quad (1)$$

where  $D$  is the exchange stiffness constant, and

$$B_t = B_{\text{int}} + B_A + B_D, \quad (2)$$

where  $B_{\text{int}} = \mu_0 H + \mu_0 M_S$  corresponds to the induction,  $B_A = \mu_0 H_A$  to the anisotropy field, and  $B_D = -\mu_0 M_S$  to the demagnetizing field. One can guess from Eq. (1) that, at a given temperature, a decrease of the applied field allows magnon modes of higher wave vector to be attainable, thus increasing the resistivity.

To account for the temperature dependence of the spin waves, the magnon mass renormalization has been introduced as

$$D \approx D_0(1 - d_1 T^2 - d_2 T^{5/2}). \quad (3)$$

The increase of the effective magnon mass with temperature has two contributions: a  $T^2$  term due to the temperature dependence of the Fermi distribution and a  $T^{5/2}$  variation expressing a higher-order corrective term due to magnon-magnon interactions.<sup>15</sup> Here  $D_0$  is the zero-temperature magnon mass,  $d_1$  and  $d_2$  being constants of the order of  $10^{-6} \text{ K}^{-2}$  and  $10^{-8} \text{ K}^{-5/2}$ , respectively, for Fe.<sup>16</sup> Due to its small amplitude, the  $d_2 T^{5/2}$  factor will be neglected.

By taking into account the high anisotropy of our samples, Raquet *et al.*'s formalism leads to the following expression for the resistivity:

$$\Delta\rho \propto \frac{B + B_A}{D(T)^2} T \ln\left(\frac{g\mu_B(B + B_A)}{kT}\right). \quad (4)$$

This equation is obviously nonlinear in  $B$ , but the variations of  $\Delta\rho$  are quasilinear when  $B_A \gg B$ . In the case of thin films of pure 3d metals,<sup>12</sup> the linearity comes from the large amplitude of the applied fields (10–30 T). In materials with strong anisotropy, such as FePt, and at low applied fields, the role of the large applied field is assumed by the anisotropy field  $B_A \gg B$ . In this way, even for low or negative applied fields, there is a linear dependence of the MMR. In order to probe our model, we measured the variation of the slope of the resistivity vs applied field, as a function of the temperature. In the case of pure 3d metals studied by Raquet *et al.*, a linear relationship to the applied field  $B$  was assumed. Derivation with respect to  $B$  (applied field) then leads to the following expression:

$$\frac{\partial \Delta\rho(T)}{\partial B} \propto T(1 + 2d_1 T^2)[\ln(T) + C^{te}], \quad (5)$$

where  $C^{te}$  is a temperature-independent term.

In our case, the applied field is low, but the linear relation has to be applied in the vicinity of the anisotropy field  $B_A$  instead of the applied field. This leads to an identical relation with the form of Eq. (5), where the constant, which is temperature independent, has the following expression:

$$C^{te} = -\ln\left(\frac{g\mu_B B_A}{k}\right) - 1 - \frac{B}{B_A} + \frac{1}{2}\left(\frac{B^2}{B_A^2}\right) + \dots \quad (6)$$

In order to confirm the variation of the MMR slope vs  $T$ , room- to low-temperature resistivity measurements on an FePt(32 nm)/MgO sample were performed using a superconducting magnet (8 T) transport setup (see Fig. 2). As expected, the MMR effect is stronger at high temperatures. The

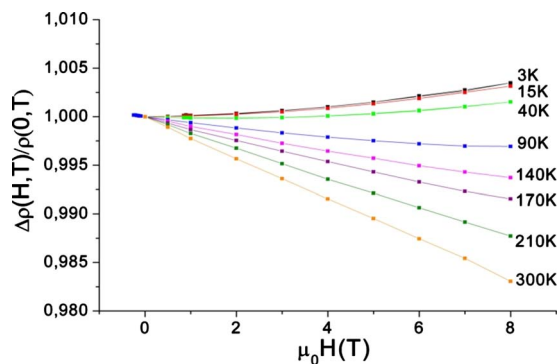


FIG. 2. (Color online) Low- to room-temperature magnetoresistance measurements performed on an FePt(32 nm)/MgO(001) sample. The resistivity values are normalized by their values at zero field.

calculated values of the slopes are plotted vs temperature in Fig. 3. By introducing a value of  $B_A = 10$  T,<sup>9</sup> the expression (5) leads to a good fit of the data (Fig. 3, solid line) with a second term  $d_1 = 1 \times 10^{-5} \text{ K}^{-2}$ .

Now that we have explained the linear dependence of the resistivity at low fields, let us focus on the resistivity decrease associated with the transition from one state of magnetization to the other. This transition between two saturated magnetization states occurs by nucleation of a few reversed domains, followed by domain wall propagation over the whole layer.<sup>9</sup> Due to the large size of the involved domains, the contribution of the domain-wall-related resistances (DWR and AMR) can be neglected in all states corresponding to partial magnetization reversal. The sample, which is much larger than the equilibrium domain size (100 nm), provides two different contributions to the MMR, arising, respectively, from the unreversed and reversed domains. The relative proportions of the area covered by the reversed and unreversed domains are given, respectively, by  $(M/M_S + 1)/2$  and  $(1 - M/M_S)/2$ . Let us denote by  $\alpha(T)$  the absolute value of the  $\rho(B)$  slope taken for a single-domain state, which can be easily obtained from measurements

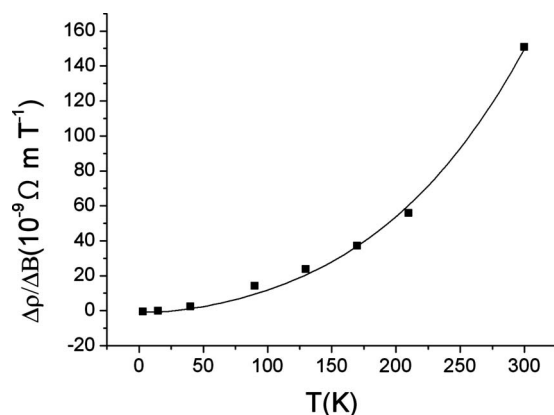


FIG. 3. Measured values (full squares) of the slope of the MMR with  $B$  vs temperature of an FePt(32 nm)/MgO(001) sample. The solid line represents a fit by Eq. (5) with a value of  $-4.32$  for the constant  $C$ .

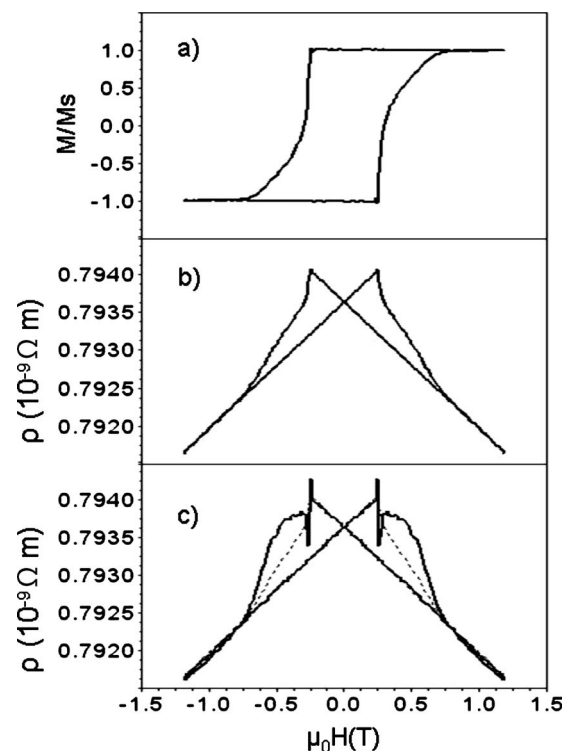


FIG. 4. (a) Hysteresis loop measured in perpendicular field by extraordinary Hall effect, (b) magnetoresistance loop calculated using  $\rho_{\text{MMR}} = -(M/M_S)\alpha(T)B$ , and (c) magnetoresistance measurement and calculated magnetoresistance (dots), performed on an FePt(32 nm)/MgO(001) sample. The difference between the pure MMR contribution (dotted part) and the actual measurement (solid line) originates from the DWR contribution to the magnetoresistance.

above the magnetization saturation. In a partially reversed state, we get

$$\rho_{\text{MMR}} = \left( -\frac{(M/M_S + 1)}{2} + \frac{(1 - M/M_S)}{2} \right) \alpha(T)B,$$

$$\rho_{\text{MMR}} = -\frac{M}{M_S} \alpha(T)B, \quad (7)$$

which implies that the MMR can be used to measure the magnetization reversal quantitatively.

This very exciting property, which had not been foreseen previously, requires some comments.

(1) The MMR signal is proportional to both magnetization and applied field, so the amplitude of the MMR effect associated with magnetization reversal is null at zero field, and increases with the applied field. As a result, magnetization reversal events corresponding to large coercive fields will provide a higher signal. In the FePt case, where the coercive field is very high, the MMR is about 0.2%, which is easily measurable using lock-in techniques, but clearly restrains this technique to fundamental studies.

(2) The MMR should be usable whenever the magnetic anisotropy implies the coexistence of two domains of opposite directions. For example, it should be usable in samples

with in-plane uniaxial anisotropy, with an in-plane applied field. It might also be measurable in nanowires where the shape anisotropy would dominate, with two in-plane magnetized domains separated by a DW, and a field applied along the wire axis. In that case, the main problem that might be encountered is that such systems usually have weak coercive fields, which implies proportionally low MMR signals.

(3) One can see directly in Fig. 1 that the MMR measurement reveals basic features of the magnetization reversal (remanence, coercive field, and so on). In our analysis, we have been able to neglect the DWR (intrinsic and AMR contributions), and straightforwardly extracted the value of  $M/M_S$  from a simple resistivity measurement. Actually, it is often necessary to take DWR into account.<sup>17</sup> In Fig. 4 we present room-temperature measurements on a thicker sample (32 nm instead of 10 nm). In this sample, the reversal is less sharp and, as the larger thickness ends up with stronger demagnetizing fields, the equilibrium size of the magnetic domain is reduced. During magnetization reversal, this implies a higher density of DWs. As a result, the DWR contribution, which is seen in Fig. 4(c), is important and cannot be neglected.

Note that in the case of nanowires reversed by a single DW, and if the DW is not too greatly deformed during its propagation, one can expect to get a constant contribution of the DWR. Moreover, if the wire is long compared to the DW's width, DWR fluctuations should be weak compared to MMR variations. Thus, in both in- and out-of-plane anisotropy, MMR measurements may allow quantitative detection of the DW position along the wire.

(4) Most experimental approaches of the DWR involve

the progressive disappearance of DWs when an external field is applied, implying that the magnetization of the sample also significantly changes. Clearly, at low  $T$ , the magnon contribution is negligible; however, this is not the case at higher temperatures. As a result, there is a modification of the contribution of the MMR to the resistance, which can be estimated quantitatively.

(5) To assess the practical implications of the MMR contribution in resistivity signals, it has to be compared to more classical magnetization reversal detection tools. It gets broadly the same kind of information (MMR proportional to  $M/M_S$ ) as the TMR and GMR, with a lower signal, but with a simpler layer structure, which can be useful in experiments where the use of multilayers would complicate the analysis of results. In comparison with the MMR, the AHE is a very accurate detection technique, but needs a more complicated geometry. Finally, the DWR offers only quantized information (the presence or not of DWs between contacts). Thus, the MMR might be in some cases the most interesting tool to detect magnetization reversal.

To sum up, the resistivity dependence on the applied field of FePt/MgO(001) thin layers highlights the presence of a magnetoresistive contribution, which can be named the magnon magnetoresistance depending not only on the applied field but also on the magnetization state. This dependence can be explained by the introduction of the anisotropy field in Raquet *et al.*'s model.<sup>12</sup> MMR measurements can thus be used as a quantitative tool to detect magnetization reversal.

\*jean-philippe.attane@cea.fr

<sup>1</sup>W. Thomson, Proc. R. Soc. London **8**, 546 (1857).

<sup>2</sup>M. N. Baibich, J. M. Broto, A. Fert, F. Nguyen Van Dau, F. Petroff, P. Etienne, G. Creuzet, A. Friederich, and J. Chazelas, Phys. Rev. Lett. **61**, 2472 (1988).

<sup>3</sup>M. Julliere, Phys. Lett. **54A**, 225 (1975).

<sup>4</sup>P. Levy and S. Zhang, Phys. Rev. Lett. **79**, 5110 (1997).

<sup>5</sup>A. Barthélemy, A. Fert, J.-P. Contour, M. Bowen, V. Cros, J. M. De Teresa, A. Hamzic, J. C. Faini, J. M. George, J. Grollier, F. Montaigne, F. Pailloux, F. Petroff, and C. Vouille, J. Magn. Mater. **242**, 68 (2002).

<sup>6</sup>A. Schuhl and D. Lacour, C. R. Phys. **6**, 945 (2005).

<sup>7</sup>A. Gerber, A. Milnera, M. Karpovskya, B. Lemkeb, H.-U. Habermeyer, J. Tuaillon-Combesc, M. Ngrierc, O. Boisronc, P. Mèlinon, and A. Perezc, J. Magn. Mater. **242**, 90 (2002).

<sup>8</sup>D. Halley, Y. Samson, A. Marty, P. Bayle-Guillemaud, C. Beigne, B. Gilles, and J. E. Mazille, Phys. Rev. B **65**, 205408 (2002).

<sup>9</sup>J. P. Attané, Y. Samson, A. Marty, D. Halley, and C. Beigne, Appl. Phys. Lett. **79**, 794 (2001).

<sup>10</sup>J. P. Attané, Y. Samson, A. Marty, J. C. Toussaint, G. Dubois, A. Mougins, and J. P. Jamet, Phys. Rev. Lett. **93**, 257203 (2004).

<sup>11</sup>J. P. Attané, D. Ravelosona, A. Marty, Y. Samson, and C. Chappert, Phys. Rev. Lett. **96**, 147204 (2006).

<sup>12</sup>B. Raquet, M. Viret, E. Sondergard, O. Cespedes, and R. Mamy, Phys. Rev. B **66**, 024433 (2002).

<sup>13</sup>D. A. Goodings, Phys. Rev. **132**, 542 (1963).

<sup>14</sup>A. G. Gurevitch and G. A. Melkov, *Magnetization Oscillations and Waves* (CRC Press, Boca Raton, FL, 1996).

<sup>15</sup>J. Mathon and E. P. Wohlfarth, Proc. R. Soc. London, Ser. A **302**, 409 (1968).

<sup>16</sup>M. W. Stringfellow, J. Phys. C **2**, 950 (1968).

<sup>17</sup>R. Danneau, P. Warin, J. P. Attané, I. Petej, C. Beigne, C. Fermon, O. Klein, A. Marty, F. Ott, Y. Samson, and M. Viret, Phys. Rev. Lett. **88**, 157201 (2002).